
NEURAL KOOPMAN LYAPUNOV CONTROL *

Vrushabh Zinage
 Graduate Student
 University of Texas at Austin
 Austin, Texas, USA
 vrushabh.zinage@utexas.edu

Efstathios Bakolas
 Associate Professor
 University of Texas at Austin
 Austin, Texas, USA
 bakolas@austin.utexas.edu

ABSTRACT

Learning and synthesizing stabilizing controllers for unknown nonlinear systems is a challenging problem for real-world and industrial applications. Koopman operator theory allow one to analyze nonlinear systems through the lens of linear systems and nonlinear control systems through the lens of bilinear control systems. The key idea of these methods, lies in the transformation of the coordinates of the nonlinear system into the Koopman observables, which are coordinates that allow the representation of the original system (control system) as a higher dimensional linear (bilinear control) system. However, for nonlinear control systems, the bilinear control model obtained by applying Koopman operator based learning methods is not necessarily stabilizable and therefore, the existence of a stabilizing feedback control is not guaranteed which is crucial for many real world applications. Simultaneous identification of these stabilizable Koopman based bilinear control systems as well as the associated Koopman observables is still an open problem. In this paper, we propose a framework to identify and construct these stabilizable bilinear models and its associated observables from data by simultaneously learning a bilinear Koopman embedding for the underlying unknown nonlinear control system as well as a Control Lyapunov Function (CLF) for the Koopman based bilinear model using a learner and falsifier. Our proposed approach thereby provides provable guarantees of global asymptotic stability for the nonlinear control systems with unknown dynamics. Numerical simulations are provided to validate the efficacy of our proposed class of stabilizing feedback controllers for unknown nonlinear systems.

Keywords Koopman operator · Neural networks · Control Lyapunov functions · Physics-informed neural networks

1 Introduction

Recently, Koopman operator techniques have proven to be powerful tools for the analysis and control of nonlinear systems whose dynamics may not be known a priori. The key idea of such methods is to associate a nonlinear system (nonlinear control system) with a linear system (bilinear control system) of higher dimension than the original system. The higher dimensional state spaces of these “lifted” linear or bilinear control systems are spanned by functions of states known as Koopman observables. Unlike linearization techniques, Koopman operator methods provide higher dimensional (lifted) linear or bilinear state space models which explicitly account for nonlinearities in the original system dynamics and their validity is not limited to a small neighborhood around a reference point or trajectory as in standard linearization approaches. However, since the Koopman operator is infinite-dimensional (which implies that the lifted state space is also infinite dimensional), the control design can become computationally intractable. In order to improve computational tractability, recent methods of Koopman operator theory (KOT) can offer a finite approximation of the operator via data-driven methods like Extended Dynamic Mode Decomposition (EDMD). EDMD mainly uses time series data to form a higher dimensional linear (bilinear) state space model that approximates the unknown nonlinear system (nonlinear control system). In addition, the connection of EDMD with Koopman operator theory has been explored in [1] and extended to non-sequential time series data in [2]. Further [3] shows the convergence

*Vrushabh Zinage (graduate student) and Efstathios Bakolas (Associate Professor) are with the Department of Aerospace Engineering and Engineering Mechanics, The University of Texas at Austin, Austin, Texas 78712-1221, USA, Emails: vrushabh.zinage@utexas.edu; bakolas@austin.utexas.edu

in the strong operator topology of the Koopman operator computed via EDMD [4] to the actual Koopman operator as the number of data points and the number of observables tend to infinity. Koopman operator theory (KOT) have been applied to robotics applications [5, 6, 7, 8, 9], power grid stabilization [10, 11], state estimation [12, 13], control synthesis [14, 15, 16, 17], actuator and sensor placement [18], aerospace applications [19, 20], analysis of climate, fluid mechanics, human-machine systems [21], chemical process systems [22] and control of PDEs. Koopman operator theory postulates that a nonlinear uncontrolled system can be lifted to an equivalent (infinite-dimensional) linear system whereas a nonlinear control system to a bilinear control system. The major challenge in realizing this lifting process is that the Koopman observables are unknown and their characterization can be a complex task. [23] presents a deep learning framework for learning the Koopman observables for uncontrolled dynamical systems. However, the learned Koopman operator is not guaranteed to be stable. [24] proposes a method to guarantee stability by learning a stable Koopman operator by utilizing a particular operator parameterization that ensures that the computed Koopman operator is Schur stable. Further, [25, 26, 27] propose data-driven approaches for identification of Koopman invariant subspaces whose applicability is, however, limited to uncontrolled nonlinear systems.

There has been a wide interest in control design methods for various robotic applications which are based on neural networks. Most of the proposed approaches in the relevant literature use reinforcement learning. However, there are no theoretical guarantees that the designed control system is stabilizable² which is crucial for safety critical applications. Towards this aim, the notion of Control Lyapunov function (CLF), which is a powerful tool from control theory, plays a vital role in characterizing and guaranteeing stability for nonlinear control systems. CLFs were first studied by Sontag [28] and Artstein during approximately the same time [29]. The existence of a CLF provides necessary and sufficient conditions to guarantee the closed-loop stability of nonlinear control systems and can be viewed as stability or safety certificates for such systems. In the control literature, there exist many approaches for the computation of Lyapunov functions for nonlinear systems based on, for instance, sum-of-squares (SOS) and semidefinite programming (SDP) optimization [30, 31, 32, 33]. However, these methods do not typically scale well and thus they cannot be applied to general high-dimensional nonlinear systems. Further, [34] showed that for a particular dynamical system, there does not exist any polynomial Lyapunov function despite the dynamical system being globally asymptotic stable.

Finding a Lyapunov function for a nonlinear system is in general a challenging task. Recently, the so-called Lyapunov neural networks methods have been proposed to learn a valid Lyapunov function that will guarantee closed-loop stability of nonlinear systems. The candidate Lyapunov functions are parameterized by means of feedforward neural networks and the Lyapunov conditions are imposed as soft constraints in the learning (optimization) problem. They are motivated by the fact that any continuous function can be approximated by means of a neural network with a finite number of parameters that must be learned [35, 36]. The Lyapunov conditions have to be satisfied for a Lyapunov function to exist. One can verify whether a neural network satisfies these conditions or not by utilizing techniques that can check certain properties of the outputs of the neural network. They can be broadly classified into two main methods, one in which the verification is inexact and is carried out by solving a relaxed convex problem and another one in which the verification is exact and based on Mixed Integer Programming (MIP) solvers and Sequential Modulo Theories (SMT) solvers. In [37, 38, 39, 40], a control strategy based on the Lyapunov function was proposed using Lyapunov neural networks. [41] proposes formal synthesis methods for learning Lyapunov functions. However, the approaches proposed in [37, 38, 39, 40, 41], assume that the nonlinear dynamics are known. [42] proposes a framework for learning a Lyapunov function where the dynamics are not known. [43] provides stability certificates via a learned Lyapunov function using trajectory data only. [44] proposes a framework for discrete-time polynomial (nonlinear) systems and learns a safe region of attraction (ROA) using neural networks. However, these approaches are restricted to learning a class of linear feedback controllers or neural network based feedback controllers and do not guarantee the existence of a stabilizing feedback controller or propose a systematic method to characterize it. Further, there are no tools to analyze these unknown nonlinear systems. In contrast with the aforementioned references, in this work we utilize the Koopman operator theory framework to describe, analyze and control the behavior of any known or unknown nonlinear system via a higher dimensional (lifted) bilinear control system.

Contributions: The main contribution of our work is four-fold. First, we propose a deep learning framework for simultaneously learning a stabilizable bilinear (lifted) state space model and the Koopman observables from data obtained from the open-loop trajectories of the latter system generated by random control inputs applied to the unknown nonlinear system. In our approach, closed-loop stability is guaranteed when our method can successfully learn a Control Lyapunov Function (CLF). Second, based on the learned CLF, we design a feedback controller using the celebrated universal Sontag’s formula [28] that guarantees closed-loop asymptotic stability. Third, our approach allows us to utilize state-of-the-art tools for verification based on SMT solvers even for unknown nonlinear dynamics by converting an unknown nonlinear system to a known higher dimensional bilinear system via Koopman operator theory in contrast with current approaches whose applicability is limited to systems with known nonlinear dynamics. Further, [45] shows the existence of a finite dimensional bilinear control system that can approximate any nonlinear control system with

²A system is stabilizable if there exists a feedback controller that can render the closed-loop system asymptotically stable

an arbitrary precision in principle. Last, in contrast to recent methods [37, 38, 39, 40, 41, 42], which assume and restrict themselves to the class of linear feedback controllers or learn a nonlinear feedback controller represented by a neural network, our method guarantees the existence of a stabilizing feedback controller which can asymptotically steer the system to origin. To the best knowledge of the authors, this is the first paper that proposes a method that simultaneously learns the Koopman operator based observables together with a stabilizable Koopman Bilinear Form (KBF) which allows us to design stabilizing feedback controllers for unknown nonlinear systems. To illustrate and also validate the ability of our proposed class of stabilizing feedback controllers to steer nonlinear systems with unknown dynamics to the desired final state, we performed numerical experiments for nonlinear control systems used in practical applications (e.g., cart poles and spacecraft) as well as popular academic examples (e.g., Van Der Pol oscillator and pendulum systems).

2 Preliminaries and Problem Statement

Consider a control-affine nonlinear system given by

$$\dot{\mathbf{x}} = F(\mathbf{x}, \mathbf{u}) = f(\mathbf{x}) + g(\mathbf{x})\mathbf{u} = f(\mathbf{x}) + \sum_{i=1}^m g_i(\mathbf{x})u_i, \quad \mathbf{x}(0) = \mathbf{x}_0 \quad (1)$$

where f is Lipschitz continuous, $g = [g_1, g_2 \dots g_m]$, where $g_i : \mathbb{R}^n \rightarrow \mathbb{R}^n$ for all $i \in [1, \dots, m]$, is assumed to be continuously differentiable, $\mathbf{x} \in \mathcal{X} \subset \mathbb{R}^n$ is the state of the system and $\mathbf{u} = [u_1, u_2, \dots, u_m]^T \in \mathcal{U} \subset \mathbb{R}^m$ is the control input applied to the system where \mathcal{X} and \mathcal{U} are compact sets. The function f is commonly known as the drift term (or vector field) whereas g is known as the actuation effect (or control vector field). Without loss of generality, we assume that the origin $\mathbf{x} = 0$ is the unique equilibrium of the uncontrolled system $\dot{\mathbf{x}} = f(\mathbf{x})$ (in other words, $\mathbf{x} = 0$ is the unique solution to the equation: $f(\mathbf{x}) = 0$) which is also assumed to be unstable. Further, we assume that $f(\mathbf{x})$ and $g(\mathbf{x})$ are unknown in general. Next, we consider a discrete-time nonlinear dynamical system which is obtained from the continuous-time system (1) after using a fourth order Runge-Kutta method:

$$\mathbf{x}_{k+1} = h(\mathbf{x}_k, \mathbf{u}_k), \quad \mathbf{x}_1(0) = \mathbf{x}_0 \quad (2)$$

where $\mathbf{x}_k \in \mathcal{D}$, $h : \mathcal{D} \rightarrow \mathbb{R}^n$, $\mathcal{D} \subset \mathbb{R}^n$ is an open set where $0 \in \mathcal{D}$. This discrete-time dynamical system will be used for construction of a dataset which would be used for training of the neural network (Section 3).

2.1 Koopman operator theory

In 1931, B. O. Koopman proved the existence of an infinite dimensional linear operator that can describe the evolution of functions of states of a nonlinear system, which are known as the observable functions (or simply observables) [46]. Formally, let \mathcal{F} be the space of functions spanned by the observables $\Phi : \mathbb{R}^n \rightarrow \mathbb{R}^N$, where $\Phi = [\phi_1, \phi_2, \dots, \phi_N]^T$ and $N > n$, then the Koopman operator $\mathcal{K} : \mathcal{F} \rightarrow \mathcal{F}$ is a linear infinite-dimensional operator that acts on functions $\Phi \in \mathcal{F}$ and is defined as follows:

$$\mathcal{K}[\Phi(\mathbf{x})] = \Phi \circ \mathcal{M}_t(\mathbf{x}), \quad (3)$$

where \mathcal{M}_t denotes the flow map of the uncontrolled nonlinear dynamics $\dot{\mathbf{x}} = f(\mathbf{x})$ which is given by

$$\mathcal{M}_t(\mathbf{x}(t_0)) = \mathbf{x}(t_0) + \int_{t_0}^{t_0+t} f(\mathbf{x}(\tau))d\tau. \quad (4)$$

It can be easily verified that \mathcal{K} is a linear operator, that is, $\mathcal{K}[k_1\Phi_1 + k_2\Phi_2] = k_1\mathcal{K}[\Phi_1] + k_2\mathcal{K}[\Phi_2]$ for all $k_1, k_2 \in \mathbb{R}$ and $\Phi_1, \Phi_2 \in \mathcal{F}$. In order to improve computational tractability, the Koopman operator is approximated by a finite-dimensional (truncated) operator which is subsequently used for modelling, control and estimation applications. For control-affine nonlinear systems described by (1), the time derivative of the observable function Φ along the system trajectories is given by the Lie derivative as follows:

$$\dot{\Phi}(\mathbf{x}) = \nabla\Phi(\mathbf{x})[f(\mathbf{x}) + g(\mathbf{x})\mathbf{u}] = \nabla\Phi(\mathbf{x})f(\mathbf{x}) + \nabla\Phi(\mathbf{x})g(\mathbf{x})\mathbf{u} = \mathcal{K}[\Phi(\mathbf{x})] + \nabla\Phi(\mathbf{x}) \sum_{i=1}^m g_i(\mathbf{x})u_i. \quad (5)$$

Let us denote by $G_i = \nabla\Phi(\mathbf{x})g_i(\mathbf{x})$. We assume that $\nabla\Phi(\mathbf{x})g_i(\mathbf{x})$ belongs to the span of $\Phi(\mathbf{x})$. In other words, there exists a constant matrix Q_i such that

$$\nabla\Phi(\mathbf{x})g_i(\mathbf{x}) = Q_i\Phi(\mathbf{x}).$$

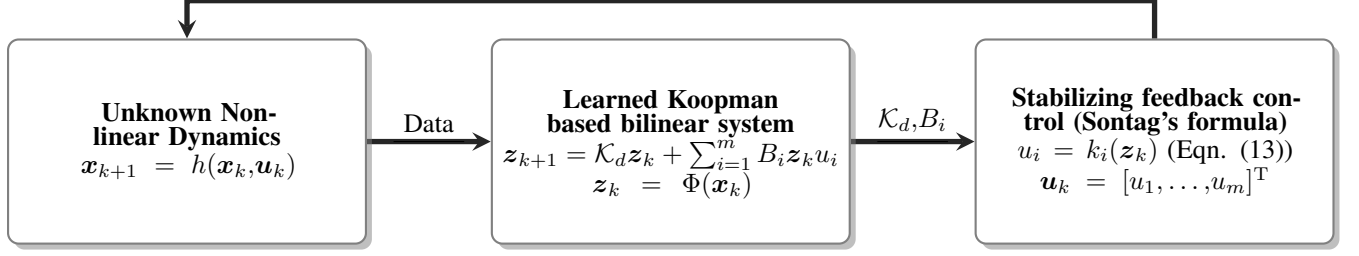


Figure 1: Learning and control framework for unknown nonlinear dynamics using Koopman operator theory

This is a reasonable assumption to make given that, as is shown in [47], for sufficiently large number of Koopman observables, the system governed by (1) can be equivalently modelled as a Koopman Bilinear Form (KBF) as follows [48]:

$$\dot{\mathbf{z}} = \mathcal{K}\mathbf{z} + \sum_{i=1}^m Q_i \mathbf{z} u_i, \quad (6)$$

where $\mathbf{z} := \Phi(\mathbf{x})$ and $\mathbf{z} \in \mathcal{X}_z$ where $\mathcal{X}_z = \{\Phi(\mathbf{x}) : \mathbf{x} \in \mathcal{X}\}$. Note that $\mathbf{z} = 0$ is a equilibrium point for the bilinear system (6). After applying Euler discretization to the KBF and assuming zero order hold, we get

$$\mathbf{z}_{k+1} = \mathbf{z}_k + \mathcal{K}T\mathbf{z}_k + \sum_{i=1}^m Q_i \mathbf{z}_k u_i T = \mathcal{K}_d \mathbf{z}_k + \sum_{i=1}^m B_i \mathbf{z}_k u_i, \quad (7)$$

where T is the sampling period, $\mathcal{K}_d := I + \mathcal{K}T$, I is the identity matrix and $B_i = Q_i T$. Note that the local truncation error $\ell(\mathbf{z}(t_k), \mathbf{z}_k)$ which is the norm of the difference between the continuous-time state at t_k , that is, $\ell(\mathbf{z}(t_k), \mathbf{z}_k) := \|\mathbf{z}(t_k) - \mathbf{z}_k\|$ satisfies the following upper bound:

$$\ell(\mathbf{z}(t_k), \mathbf{z}_k) \leq pLT^2, \quad (8)$$

where p , L , and T are given by

$$L := \left\| \mathcal{K}_d + \sum_{i=1}^m B_i \mathbf{z}_k u_i \right\|, \quad p = L \sup_{kT \leq t < kT+T} \|\mathbf{z}(t)\|. \quad (9)$$

Note that the truncation error tends to zero as T tends to zero. Hence even if for a given T , the truncation error between the states of the discrete-time and continuous-time systems is not sufficiently small, T can be reduced accordingly. Note that in contrast to discretization approaches like Runge-Kutta, the Euler discretization preserves the bilinear form in the discrete-time domain. This was the main motivation as to why Euler discretization was chosen over the Runge-Kutta method.

Remark 1 Of particular interest, is that if one would be able to find Koopman observables such that the nonlinear system can be represented by linear time invariant systems as follows:

$$\dot{\mathbf{z}} = A\mathbf{z} + B\mathbf{u} \quad (10)$$

which can be expressed in discrete-time form via exact discretization as follows:

$$\mathbf{z}_{k+1} = A_d \mathbf{z}_k + B_d \mathbf{u}_k, \quad (11)$$

where $A_d = e^{AT}$, $B_d = \int_0^T e^{At} dt B$ and T is the sampling period. Recently, the approach of lifting a nonlinear control system to a linear control system has gained a lot of attention due to the availability of rich libraries of tools to analyze and design controllers for linear systems. However, it should be noted that lifting a nonlinear system into a higher dimensional linear system can be quite restrictive in practice because it may be hard to find a linear system that accurately describe the behavior of the original nonlinear system as pointed out in [49]. Further, the realization of the Koopman operator based lifting process when applied to a control-affine nonlinear system corresponds to a bilinear control system rather than a linear system. This (lifted) bilinear representation of the control-affine nonlinear system has several advantages over the Koopman based linear representation as pointed out in [50].

2.2 Existence of stabilizing feedback controller

For the control-affine bilinear system given by (6), let us define a continuously differentiable positive definite function $V : \mathcal{D} \rightarrow \mathbb{R}_+$ (V is positive everywhere except at $z = 0$ where it is zero) such that the infimum of Lie derivative of V over all inputs is negative. More precisely,

$$\inf_{u \in \mathcal{U}} \dot{V}(z) < 0 \quad (12a)$$

$$\text{where } \dot{V}(z) := \frac{\partial V}{\partial z} \dot{z} = \frac{\partial V}{\partial z} \mathcal{K}z + \frac{\partial V}{\partial z} \sum_{i=1}^m Q_i z u_i. \quad (12b)$$

If the infimum of the Lie derivative of the CLF over all $u \in \mathcal{U}$ is negative, then there exists a control input for which $\dot{V}(z)$ is negative along the trajectories of the closed-loop system. In particular, it can be shown that in the latter case there exists a feedback controller $u := k(z) = [k_1(z), \dots, k_m(z)]^T$ that renders the system globally asymptotically stable (in other words, $k(z)$ is a globally stabilizing feedback controller). This is stated formally as follows:

Theorem 1 [51] For the system given by (6), there exists a continuously differentiable function $k(z)$ for all $z \in \mathbb{R}^N \setminus \{0\}$ and continuous at $z = 0$ such that the controller $u = k(z)$ renders the zero solution $z = 0$ of the closed-loop system globally asymptotically stable if and only if there exists a radially unbounded Control Lyapunov function (CLF) $V(z)$ such that

(C1) For all $z \neq 0$, $\sum_{i=1}^m \frac{\partial V}{\partial z} Q_i z u_i = 0$ implies $\frac{\partial V}{\partial z} \mathcal{K}z < 0$

(C2) For all $\epsilon > 0$, there exists $\delta > 0$ such that $\|z\| < \delta$ implies the existence of $\|u\| < \epsilon$ satisfying (12)

The condition (C2) is also known as the small control property. If both conditions (C1) and (C2) hold true, then the stabilizing control input $u := k(z) = [k_1(z), k_2(z), \dots, k_m(z)]^T$, where the i -th component $k_i(z)$ of the feedback controller $k(z)$ satisfies the universal Sontag's formula [28]:

$$k_i(z) = \begin{cases} -\frac{c_i(z)[a(z) + \sqrt{a^2(z) + \sigma^2(z)}]}{\sigma(z)}, & \text{if } \sigma(z) \neq 0 \\ 0, & \text{otherwise} \end{cases} \quad (13)$$

where $a(z) = \frac{\partial V}{\partial z} \mathcal{K}z$, $\sigma(z) = \sum_{i=1}^m (\frac{\partial V}{\partial z} Q_i z u_i)^2$, and $c_i(z) = \frac{\partial V}{\partial z} Q_i z$.

Remark 2 In contrast to recent methods which assume a linear feedback controller [37, 40] or a nonlinear feedback controller represented by a neural network [42], our approach guarantees the existence of a stabilizing controller that asymptotically steers the unknown nonlinear system (1) to origin.

2.3 Problem statement

In this paper, we address the following problem:

Problem 1 Given the data snapshots X from the unknown nonlinear control system (1), compute the Koopman observables $z = \Phi(x)$ and the matrices $[\mathcal{K}_d, B_1, \dots, B_m]$ governing the Koopman based bilinear system (6). Further, design a feedback controller that renders the zero solution of the unknown nonlinear system (1) asymptotically stable.

3 Learning Koopman operator based stabilizable bilinear control system

Let the state snapshots $\{x_k\}_{k=1}^{N_d}$ and corresponding control inputs $\{u_k\}_{k=0}^{N_d-1}$ be obtained using the discrete-time model in (2) when the control input u_k is applied to (2) to take the state from x_k to x_{k+1} for all $k \in \{1, 2, \dots, N_d - 1\}$ and let N_d denote the total number of data snapshots. Consider an encoder $z = \Phi(x; \theta) : \mathbb{R}^n \rightarrow \mathbb{R}^N$ which maps the state $x \in \mathbb{R}^n$ to a higher dimensional lifted state $z \in \mathbb{R}^N$ where $N > n$ and θ denotes the vector of parameters of the neural network. Similarly, let $x = \Phi^{-1}(z; \theta) : \mathbb{R}^N \rightarrow \mathbb{R}^n$ denote the decoder which maps the lifted state back to the original state x as shown in Fig. 2. For notational simplicity, we represent $\Phi(z; \theta)$ by $\Phi(z)$. We construct a CLF $V(z; \theta)$, to be the output of a feedforward neural network. The main motivation for using feedforward neural networks for representing CLF is that they are expressive in the sense that any continuous function can be represented by means of a feedforward network with a finite number of parameters. For notational simplicity, we denote $V(z; \theta)$ by $V_\theta(z)$. Since the CLF has to be continuously differentiable, a smooth \tanh activation function is used. One can also use the smooth approximations of the ReLU activation function. The objective is to simultaneously learn a valid CLF, Koopman observables z , the discrete-time Koopman operator \mathcal{K}_d and the matrices B_i for all $i \in \{1, 2, \dots, m\}$ that appear in the governing equations of the bilinear system by minimizing the following loss function \mathcal{L} given by

$$\mathcal{L} = \alpha_1 \mathcal{L}_{\text{recons}} + \alpha_2 \mathcal{L}_{\text{dyn}} + \alpha_3 \mathcal{L}_{\text{phy}} + \alpha_4 \mathcal{L}_{\text{lyap}} + \mathcal{L}_{\text{ROA}} \quad (14)$$

where $\alpha_1, \alpha_2, \alpha_3$ and α_4 are positive hyperparameters. Now, we describe the individual losses $\mathcal{L}_{\text{recons}}, \mathcal{L}_{\text{dyn}}, \mathcal{L}_{\text{phy}}, \mathcal{L}_{\text{lyap}}, \mathcal{L}_{\text{ROA}}$ whose weighted sum constitute the overall loss function \mathcal{L} .

Reconstruction loss $\mathcal{L}_{\text{recons}}$: The reconstruction loss ensures that the encoder is able to lift the state \mathbf{x} and the decoder is able to project back the lifted state \mathbf{z} to \mathbf{x} . The expression for $\mathcal{L}_{\text{recons}}$ is given by

$$\mathcal{L}_{\text{recons}} = \frac{1}{N_d} \sum_{k=1}^{N_d} \|\mathbf{x}_k - \Phi^{-1}(\Phi(\mathbf{x}_k))\|_2^2$$

Bilinear control system loss \mathcal{L}_{dyn} : The dynamical system loss \mathcal{L}_{dyn} (also known as the bilinear control system loss in this case) represents the extent to which the observables obey the governing Koopman based bilinear system and is given by the following expression

$$\mathcal{L}_{\text{dyn}} = \frac{1}{N_d - 1} \sum_{i=1}^{N_d-1} \left\| \Phi(\mathbf{x}_{i+1}) - \mathcal{K}_d \Phi(\mathbf{x}_i) - \sum_{j=1}^m [\mathbf{u}_i]_j B_j \Phi(\mathbf{x}_i) \right\|_2^2$$

During every epoch, the matrices $\mathcal{K}_d, B_1, \dots, B_m$ are updated as follows:

$$\begin{bmatrix} \mathcal{K}_d & B_1 & \dots & B_m \end{bmatrix} = \beta_{N_d} \Psi_{N_d}^T (\Psi_{N_d} \Psi_{N_d}^T)^{-1} \quad (15)$$

where the matrices Ψ_{N_d} and β_{N_d} are given by

$$\Psi_{N_d} = \left[\begin{pmatrix} 1 \\ \mathbf{u}_1 \end{pmatrix} \otimes \Phi(\mathbf{x}_1), \dots, \begin{pmatrix} 1 \\ \mathbf{u}_{N_d-1} \end{pmatrix} \otimes \Phi(\mathbf{x}_{N_d-1}) \right], \quad \beta_{N_d} = [\Phi(\mathbf{x}_2), \dots, \Phi(\mathbf{x}_{N_d})] \quad (16)$$

where \otimes denotes the Kronecker product. Note that for given Φ and Φ^{-1} , the matrices $\mathcal{K}, B_1, \dots, B_m$ updated as in (15) minimize \mathcal{L}_{dyn} if Ψ_{N_d} is a full row-rank matrix. This approach is known as the Extended Dynamic Mode Decomposition (EDMD). Note that Ψ_{N_d} can be made full row-rank if we increase the number of data-snapshots. Further, these matrices are updated optimally during every epoch of training the neural network. However, the major challenge is that the right Koopman observables Φ are unknown at the start. Hence, the loss initially is not zero and can actually be significantly large.

Physics-informed loss \mathcal{L}_{phy} : This loss measures the extent to which the state is away from the true underlying nonlinear dynamics and is given as follows:

$$\mathcal{L}_{\text{phy}} = \frac{1}{N_d - 1} \sum_{i=1}^{N_d-1} \left\| \Phi^{-1}(\Phi(\mathbf{x}_{i+1})) - h(\Phi^{-1}(\Phi(\mathbf{x}_i)), \mathbf{u}_i) \right\|_2^2 \quad (17)$$

Minimizing the physics-informed loss ensures that the learned bilinear model can predict states which are far away from the training data. In addition, it ensures that the encoder and the decoder respect the underlying nonlinear dynamics while simultaneously learning the Koopman based observables.

Control Lyapunov risk $\mathcal{L}_{\text{lyap}}$: The control design based on CLF involves minimizing the minimax cost which is represented as follows [37]:

$$\inf_{\theta, u \in \mathcal{U}} \sup_{\mathbf{z} \in \mathcal{X}_{\mathbf{z}}} (\max(0, -V_{\theta}(\mathbf{z})) + \max(0, \nabla V_{\theta}(\mathbf{z})) + V_{\theta}^2(0)) \quad (18)$$

where $\nabla V_{\theta}(\mathbf{z})$ (Lie derivative of $V_{\theta}(\mathbf{z})$) is defined as follows:

$$\nabla V_{\theta}(\mathbf{z}) = \frac{\partial V}{\partial \mathbf{z}} \mathcal{K} \mathbf{z} + \frac{\partial V}{\partial \mathbf{z}} \sum_{i=1}^m Q_i \mathbf{z} u_i = \frac{\partial V}{\partial \mathbf{z}} \frac{(\mathcal{K}_d - I) \mathbf{z}}{T} + \frac{\partial V}{\partial \mathbf{z}} \sum_{i=1}^m \frac{B_i \mathbf{z} u_i}{T}$$

The first term in (18) ensures that the CLF is positive definite, the second term ensures that the Lie derivative of CLF is negative and the last terms ensures that the value of CLF at origin is zero. The control Lyapunov loss function $\mathcal{L}_{\text{lyap}}$ measures the degree of violation of the Lyapunov conditions mentioned in (12). Let the value of $\inf_{\theta, u \in \mathcal{U}} \sup_{\mathbf{z} \in \mathcal{X}_{\mathbf{z}}} (\max(0, -V_{\theta}(\mathbf{z})) + \max(0, \nabla V_{\theta}(\mathbf{z})) + V_{\theta}^2(0))$ be $G(\mathbf{z}_{\text{opt}})$. If $V_{\theta}(\mathbf{z})$ is a valid CLF, then $G(\mathbf{z}_{\text{opt}}) = G(\mathbf{z}_1) = \dots = G(\mathbf{z}_{N_d}) = 0$. Since a valid CLF is not known during the training process and given

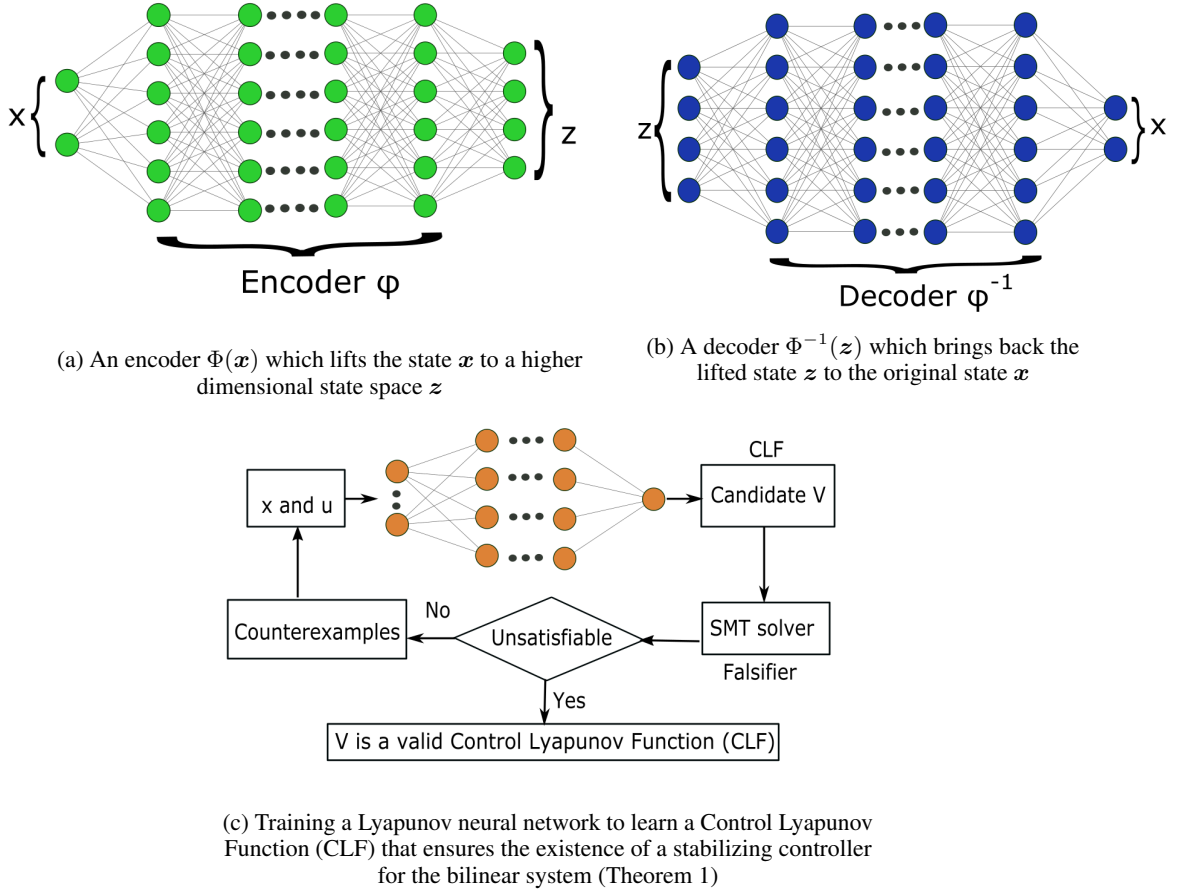


Figure 2: Deep learning framework to learn a stabilizable bilinear control system and a Control Lyapunov Function (CLF)

the set $\mathcal{Z} = \{z_1, z_2, \dots, z_{N_d}\}$, the conditional probability $\mathbb{P}(G(z_{\text{opt}}) = G(z_1) | \mathcal{Z}) = \mathbb{P}(G(z_{\text{opt}}) = G(z_2) | \mathcal{Z}) = \dots = \mathbb{P}(G(z_{\text{opt}}) = G(z_{N_d}) | \mathcal{Z})$. Therefore, the optimal unbiased Monte Carlo estimate of the control Lyapunov risk is given by the sample mean as follows:

$$\mathcal{L}_{\text{lyap}} = \frac{1}{N_d} \sum_{i=1}^{N_d} (\max(0, -V_{\theta}(z_i)) + \max(0, \nabla V_{\theta}(z_i)) + V_{\theta}^2(0)) \quad (19)$$

The violation of the Lyapunov conditions leads to failure in designing control inputs as these conditions need to be guaranteed over all states in \mathcal{D} . To avoid this issue a first-order logic (also known as the falsification constraint) is incorporated which generates a counter-example that would not satisfy the Lyapunov conditions (12). In other words, the first-order logic $\mathcal{F}_{\varepsilon}(z)$ can be represented as

$$\mathcal{F}_{\varepsilon}(z) = \left(\sum_{i=1}^N z_i^2 = \sum_{i=1}^N \Phi(x)_i^2 \geq \varepsilon > 0 \right) \wedge (V_{\theta}(z) \leq 0 \vee \nabla V_{\theta}(z) \geq 0) \quad (20)$$

To avoid numerical sensitivity issues, the value of ε is orders of magnitude smaller than the dimension of \mathcal{X}_z . Further, ε is chosen such that $\sum_{i=1}^n x_i^2 \geq \varepsilon$ would imply that $\sum_{i=1}^N z_i^2 \geq \varepsilon$. Therefore, ε is chosen such that

$$\varepsilon \ll \min \left\{ 1, \|\mathcal{X}_z\|, \min \left\{ \sum_{i=1}^n x_i^2, \sum_{i=1}^N z_i^2 \right\} \right\} \quad (21)$$

Satisfiability Modulo Theories (SMT) algorithms are used to determine whether a mathematical formula is satisfiable or not. We use a SMT algorithm for generating counterexamples which satisfy the falsification constraint. The problem of

generating examples that satisfy the nonlinear constraints is highly non-convex and is NP hard. However, recent progress among the class of SMT algorithms has shown to be effective in solving problems with such nonlinear constraints. The neural network is trained until the SMT solver is not able to generate a counterexample satisfying the falsification constraint. Once a counterexample is generated, the training data are updated accordingly to further train the neural network. Note that a SMT solver never fails to generate counterexamples which satisfy the falsification constraint if there are any. This is rigorously proved for SMT solvers such as dReal in [52].

If the dimension of the nonlinear system is large, learning a valid CLF using \mathcal{L}_{dyn} and \mathcal{F}_ε might be computational expensive for a SMT solver. Towards that aim, \mathcal{L}_{dyn} and \mathcal{F}_ε can be simplified by considering the set of candidate CLF's as follows. Consider a set of candidate Control Lyapunov Functions $V(\mathbf{z}; \theta)$ as follows:

$$V(\mathbf{z}; \theta) = \mathbf{z}^T (\gamma I + W_N(\mathbf{z})^T W_N(\mathbf{z})) \mathbf{z}, \quad (22)$$

where $W_N(\mathbf{z})$ is a $n_w \times N$ matrix that corresponds to the output of a feedforward neural network, $\gamma > 0$ and n_w is the number of hyper-parameters. Clearly, $V(\mathbf{z}; \theta)$ is positive definite given that the matrix $I + W_N(\mathbf{z})^T W_N(\mathbf{z})$ is positive definite as the sum of a positive definite matrix and a positive semi-definite matrix. Therefore, $\mathcal{L}_{\text{lyap}}$ and $\mathcal{F}_\varepsilon(\mathbf{z})$ can be written as follows:

$$\mathcal{L}_{\text{lyap}} = \frac{1}{N_d} \sum_{i=1}^{N_d} (\max(0, \nabla V_\theta(\mathbf{z}_i)) + V_\theta^2(0)), \quad \mathcal{F}_\varepsilon(\mathbf{z}) = \left(\sum_{i=1}^N \mathbf{z}_i^2 = \sum_{i=1}^N \Phi(\mathbf{x})_i^2 \geq \varepsilon \right) \wedge (\nabla V_\theta(\mathbf{z}) \geq 0)$$

Remark 3 A stabilizable Koopman based linear model can also be learned by suitably modifying \mathcal{L}_{dyn} and $\mathcal{L}_{\text{lyap}}$ as $\mathcal{L}_{\text{dyn}} = \frac{1}{N_d-1} \sum_{i=1}^{N_d-1} \|\Phi(\mathbf{x}_{i+1}) - \mathcal{K}_d \Phi(\mathbf{x}_i) - B_d \mathbf{u}_i\|_2^2$ where the matrices A_d and B_d (Eqn. (11)) are updated during epoch as follows:

$$[\mathcal{K}_d, B_d] \triangleq [A_d, B_d] = \beta_{N_d} [\Psi_{N_d}, \mathbf{U}]^\dagger \quad (23)$$

where \dagger denotes the Moore-Pseudo inverse and β_{N_d} , Ψ_{N_d} and \mathbf{U} are given by

$$\Psi_{N_d} = [\Phi(\mathbf{x}_1), \dots, \Phi(\mathbf{x}_{N_d-1})], \quad \beta_{N_d} = [\Phi(\mathbf{x}_2), \dots, \Phi(\mathbf{x}_{N_d})], \quad \mathbf{U} = [\mathbf{u}_1, \dots, \mathbf{u}_{N_d}]. \quad (24)$$

Further the control Lyapunov risk and the falsification constraint remain the same except that $\nabla V_\theta(\mathbf{z})$ now becomes:

$$\nabla V_\theta(\mathbf{z}) = \frac{\partial V}{\partial \mathbf{z}} \frac{(\mathcal{K}_d - I)\mathbf{z}}{T} + \frac{\partial V}{\partial \mathbf{z}} B \quad (25)$$

Instead of asymptotic stability, one can ensure exponential stability by suitably modifying the control Lyapunov loss $\mathcal{L}_{\text{lyap}}$ and the falsification constraint \mathcal{F}_ε as follows:

Definition 1 (Globally exponential stability): The closed-loop system is globally exponentially stable if there exists a positive continuously differentiable and radially unbounded function $V(\mathbf{z})$ and constants $\gamma_1 > 0$, $\gamma_2 > 0$, $\gamma_3 > 0$ such that

$$\gamma_1 \|\mathbf{z}\|_2^2 \leq V(\mathbf{z}) \leq \gamma_2 \|\mathbf{z}\|_2^2, \quad \dot{V}(\mathbf{z}) \leq -\gamma_3 V(\mathbf{z}) \quad (26)$$

A function V that satisfies (26) is referred as an exponentially stabilizing Lyapunov Function (or simply a Lyapunov Function). Note that if we want the Koopman bilinear system to be globally exponentially stable, then the latter requirement can be easily incorporated in the $\mathcal{L}_{\text{lyap}}$ as follows:

$$\mathcal{L}_{\text{lyap}} = \frac{1}{N_d} \sum_{i=1}^{N_d} (\max(0, \gamma_1 \|\mathbf{z}_i\|_2^2 - V_\theta(\mathbf{z}_i)) + \max(0, V_\theta(\mathbf{z}_i) - \gamma_2 \|\mathbf{z}_i\|_2^2) + \max(0, \nabla V_\theta(\mathbf{z}_i) + \gamma_3 V_\theta(\mathbf{z}_i)) + V_\theta^2(0))$$

$$\mathcal{F}_\varepsilon(\mathbf{z}) := \left(\sum_{i=1}^N \mathbf{z}_i^2 \geq \varepsilon \right) \wedge ((V_\theta(\mathbf{z}_i) - \gamma_1 \|\mathbf{z}_i\|_2^2) \leq 0 \vee (\gamma_2 \|\mathbf{z}_i\|_2^2 - V_\theta(\mathbf{z}_i)) \leq 0 \vee (\nabla V_\theta(\mathbf{z}) + \gamma_3 V_\theta(\mathbf{z})) \geq 0)$$

Region of attraction (RoA): Let $\phi(t, \mathbf{z})$ be the solution to the system of ordinary differential equations which describe the dynamics of a nonlinear system with initial condition \mathbf{z} at time $t = 0$. Then, the Region of Attraction (RoA) is defined as the set of all points such that $\lim_{t \rightarrow \infty} \phi(t, \mathbf{z}) = 0$ [53].

Finding the exact region of attraction either analytically or numerically is not possible for many practical cases. However, one can use Lyapunov based methods to estimate the RoA of nonlinear systems [54, 55]. If there exists a Lyapunov

function that satisfies the conditions of asymptotic stability over a domain \mathcal{X}_z and if $\Omega_c = \{z \in \mathbb{R}^N : V(z) \leq c\} \subset \mathcal{X}_z$. The ROA loss \mathcal{L}_{ROA} is defined as follows:

$$\mathcal{L}_{\text{ROA}} = \frac{1}{N_d} \sum_{i=1}^{N_d} \|z_i\|_2 - \gamma_4 V_\theta(z_i) \quad (27)$$

where $\gamma_4 > 0$ is a tunable parameter. The region of attraction is also called as the region of asymptotic stability or domain / basin of attraction [53].

Remark 4 Although, the optimization problem (i.e., minimizing the loss given in (14)) is highly non-convex, recent results in deep learning have been successful in finding global minima for solving these non-convex problems.

The overall algorithm used to learn and control an unknown nonlinear system is described in Algorithm 1. Its main steps can be summarized as follows. The function **LEARNING** takes the data snapshots and returns the learned matrices governing the higher dimensional bilinear system, Koopman observables (encoder), decoder and a valid CLF. The learned CLF and the matrices governing the bilinear systems are then used to design a stabilizing feedback controller based on Sontag’s formula (13). The function **CONTROL** takes the initial state x_0 and computes the control sequence U (via the learned Koopman based bilinear model and the Control Lyapunov function) which steers the unknown nonlinear control system to the origin.

Algorithm 1 Learning Koopman operator based stabilizable bilinear model for control

```

Input:  $N_d, n, m, T, X = \{x_k, u_k\}_{k=1}^{N_d}$ 
Output:  $\Phi, \Phi^{-1}, \mathcal{K}_d, B_i \forall i \in \{1, \dots, m\}, u = k(z)$ 

1: function LEARNING( $\{x_k\}_{k=1}^{N_d}, \{u_k\}_{k=1}^{N_d}$ )
2:   Repeat:
3:      $\Phi, \Phi^{-1} \leftarrow \text{NN}_\theta(x, z)$  ▷ Encoder and decoder
4:      $V_\theta(z) \leftarrow \text{NN}_\theta(z)$  ▷ Candidate Control Lyapunov Function (CLF)
5:      $[\mathcal{K}_d, \dots, B_m] \leftarrow \beta_{N_d} \Psi_{N_d}^T (\Psi_{N_d} \Psi_{N_d}^T)^{-1}$  ▷ Update bilinear system matrices
6:      $\nabla V_\theta(z) \leftarrow \frac{\partial V}{\partial z} \frac{(\mathcal{K}_d - I)z}{T} + \frac{\partial V}{\partial z} \sum_{i=1}^m \frac{B_i z u_i}{T}$ 
7:     Compute total loss  $\mathcal{L}(\theta)$  from Eqn. (14)
8:      $\theta \leftarrow \theta + \alpha \nabla_\theta \mathcal{L}(\theta)$  ▷ Update weights
9:   until convergence
10:  return  $\Phi, \Phi^{-1}, [\mathcal{K}_d, \dots, B_m], V_\theta(z)$ 
11: end function
12: function FALSIFICATION( $X$ )
13:  Impose conditions defined in Eqn. (20)
14:  Use SMT solver to verify the conditions
15:  return satisfiability
16: end function
17: function CONTROL( $x_0$ ) ▷ Stabilizing feedback controller
18:   $\Phi, \Phi^{-1}, [\mathcal{K}_d, \dots, B_m], V_\theta(z) \leftarrow \text{LEARNING}(X)$ 
19:  Repeat:
20:     $u \leftarrow \text{Eqn. (13)}, U \leftarrow \text{Append}(u)$  ▷ Universal Sontag’s formula
21:     $x_{\text{next}} \leftarrow \text{Apply feedback control law } u \text{ to discrete system (Eqn. (2))}$  ▷ Propagate the state
22:     $x \leftarrow x_{\text{next}}$ 
23:  until convergence
24:  return  $U$ 
25: end function
26: function MAIN()
27:  while Satisfiable do
28:    Add counterexamples to  $X$ 
29:     $\Phi, \Phi^{-1}, [\mathcal{K}_d, \dots, B_m], V_\theta(z) \leftarrow \text{LEARNING}(X)$ 
30:     $S \leftarrow \text{FALSIFICATION}(X)$ 
31:  end while
32:   $U \leftarrow \text{CONTROL}(x_0)$ 
33: end function

```

4 Results

In this section, we present the experimental results of our proposed approach on various nonlinear control problems. The learning framework is implemented in PyTorch for the simulations and our implementation follows Algorithm 1. The

dReal package (SMT solver) is used to generate counterexamples for learning a valid CLF. The code for the numerical experiments can be found at <https://github.com/Vrushabh27/Neural-Koopman-Lyapunov-Control>. In contrast to the approach proposed in [37, 38, 39, 40, 41, 42], the main advantage of using our proposed method is two-fold. First, Koopman operator theory allows us to analyze a unknown nonlinear system via a learned higher dimensional Koopman based bilinear system. Second, unlike recent methods which restrict themselves to linear feedback controllers or learn a neural network based controller, our approach provides provable guarantee for the existence of a stabilizing controller for the unknown nonlinear system.

The training was performed for at least 900 epochs with Adam optimizer before the falsifier was used to generate counterexamples (that violate CLF conditions) which were then added to the training data. The activation function used for the encoder, decoder and the CLF is Tanh with learning rate set to 10^{-3} and the Mean Squared Error (MSE) loss for all the examples. The analytical expressions for $V_\theta(z)$ and $\Phi(x)$ are required to generate counterexamples by a SMT verifier (falsifier (20)) and compute the feedback stabilizing controller (Eqn. (13)). The expressions for $V_\theta(z)$ and $\Phi(x)$ are represented by the following recursive relations:

$$\begin{aligned} \text{CLF: } V_\theta(z) &= \tanh(W_{h^v+1}^v y_{i+1} + b_{h^v+1}^v) \quad \text{where } y_i = \tanh(W_i^v y_{i-1} + b_i^v), \quad i = h^v, \quad y_1^v = z \\ \text{Encoder: } \Phi(x) &= \tanh(W_{h^e+1}^e y_{i+1} + b_{h^e+1}^e) \quad \text{where } y_i = \tanh(W_i^e y_{i-1} + b_i^e), \quad i = h^e, \quad y_1^e = x \end{aligned}$$

where h^v , W_i^v , b_i^v and h^e , W_i^e , b_i^e denote the number of hidden layers, weights and biases of the CLF and encoder respectively. In order to train the encoder, decoder and the CLF, we assume that a black-box simulator of the unknown nonlinear dynamics (2) is available where x_{k+1} is returned given x_k and u_k .

For the pendulum system and the Van Der Pol oscillator, we use the encoder and CLF with 1 hidden layer of 6 units each whereas for the cart pole system and the spacecraft rendezvous problem, we use the encoder and CLF with 2 hidden layers of 32 units each. For the decoder, we use a neural network with 2 hidden layers of 16 units each for all experiments.

Hyperparameter tuning; The hyperparameters α_1 , α_2 , α_3 and α_4 were tuned based on the combination of the controller performance and the empirical loss on the training data. We observed that for the pendulum and Van Der Pol system, $\alpha_1 = \alpha_3 = 0.001$, $\alpha_2 = 2$ and $\alpha_4 = 1$ yielded best results whereas for the cart pole and spacecraft rendezvous system we obtained the best results for $\alpha_1 = \alpha_3 = 0.05$, $\alpha_2 = 3$ and $\alpha_4 = 1$.

In the following subsections, we consider two popular academic nonlinear systems followed by two real world nonlinear systems.

4.1 Pendulum system

The pendulum dynamics is given by

$$\dot{x}_1 = x_2, \quad \dot{x}_2 = -\frac{mg}{l}\sin(x_1) + u \quad (28)$$

where $x = [x_1, x_2]^T$ is the state, u is the control input, m and l is the mass and length of the pendulum respectively. We set the sampling time T to be 0.005s. Note that the origin corresponds to an equilibrium of the pendulum system in the control-free case. The state domain $\mathcal{X} = \{x : x_{lb} \leq x \leq x_{ub}\}$ where $x_{lb} = [-1, -1]^T$ and $x_{ub} = [1, 1]^T$. Figs. 3a and 3b shows the evolution of the ten trajectories whose initial conditions are randomly sampled from \mathcal{X} and Fig. 3c shows the evolution of the stabilizing control inputs (based on the learned CLF, Koopman observables z and Sontag's formula (13)) which were applied to these trajectories. Fig. 3d shows the trajectories in the phase space.

4.2 Van Der Pol oscillator

Next, we consider the Van Der Pol oscillator system whose governing equations are given by

$$\dot{x}_1 = x_2, \quad \dot{x}_2 = (1 - x_1^2)x_2 + x_1 + u \quad (29)$$

where $x = [x_1, x_2]^T \in \mathbb{R}^2$ is the state and $u \in \mathbb{R}$ is the control input for the Van Der Pol oscillator. We define the state domain $\mathcal{X} = \{x : x_{lb} \leq x \leq x_{ub}\}$ (the inequality denotes the element wise comparison) where $x_{lb} = [-10, -10]^T$ and $x_{ub} = [10, 10]^T$. We set the sampling time $T = 0.01$. Figs. 4a and 4b show the evolution of the states of the Van Der Pol oscillator with initial conditions x_0 sampled from the set \mathcal{X} . Once a valid CLF is learned from training the neural network, it is used in the Sontag's formula to design a stabilizing feedback controller that would steer the state from x_0 to origin.

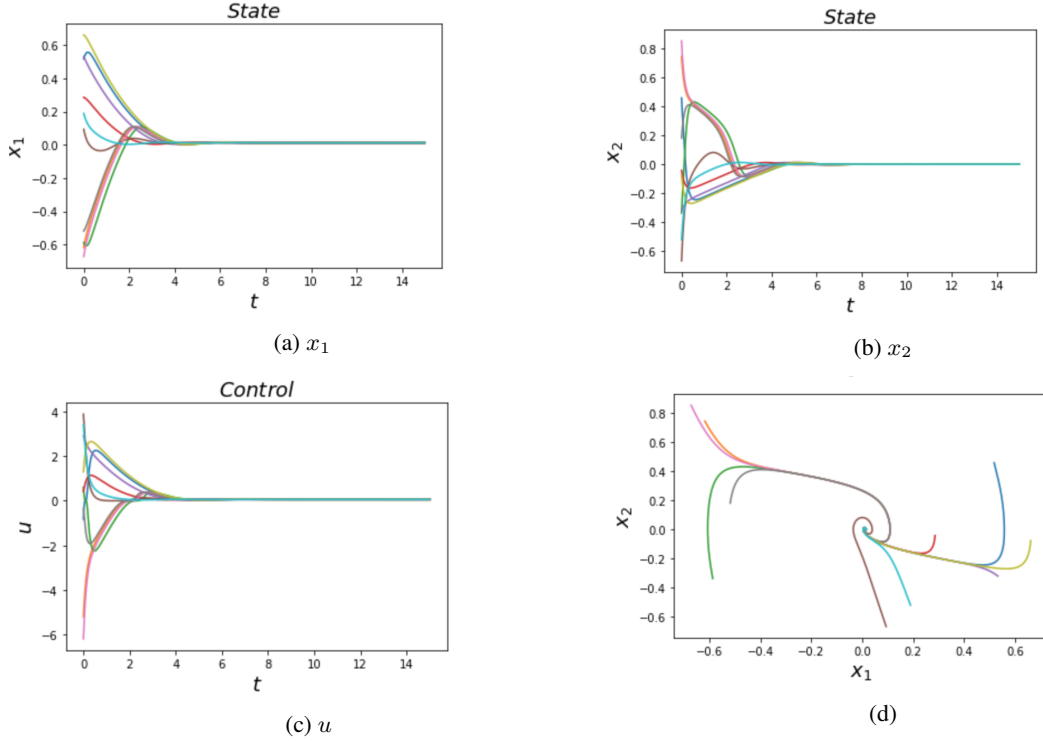


Figure 3: The evolution of the state and control input with time for the pendulum system

The control inputs are shown in Fig. 4c. Note that the origin is the unstable equilibrium. If no control input is applied, the trajectories will converge to a limit cycle (shown by green dotted curve in Fig. 4d), irrespective of the initial state.

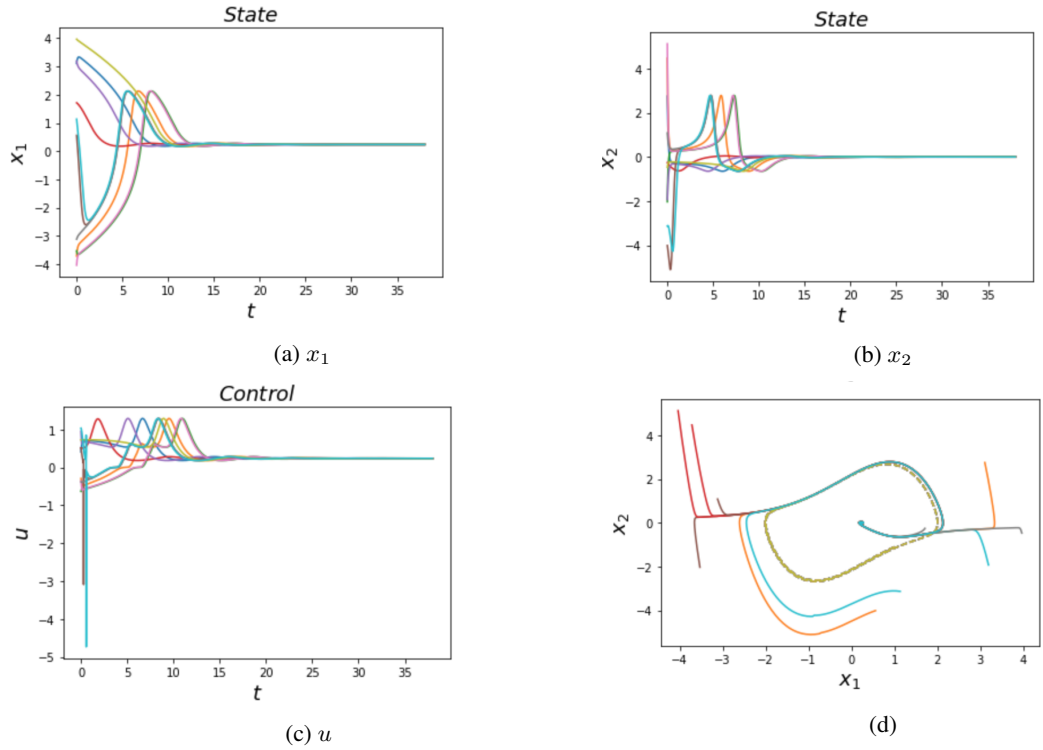


Figure 4: The evolution of the state and control input with time for the Van Der Pol oscillator

4.3 Cart pole system

The cart pole system is a fully underactuated system with one control input and two degrees of freedom (DOF). Due to its highly nonlinear structure, it is used to validate nonlinear controllers. Cart pole systems can find many applications such as rocket propellers, self balancing robots, stabilization of ships etc. The cart pole dynamics is given as follows:

$$\dot{x} = \frac{u + m_p \sin \theta (l \dot{\theta}^2 - g \cos \theta)}{m_c + m_p (\sin \theta)^2}, \quad \ddot{\theta} = \frac{u \cos \theta + m_p l \dot{\theta}^2 \cos \theta \sin \theta - (m_c + m_p) g \sin \theta}{l (m_c + m_p (\sin \theta)^2)} \quad (30)$$

where $m_c = 4$ is the mass of the cart, $l = 1$ and $m_p = 1$ are the length and mass of the pole respectively, $x = [x_1, x_2, x_3, x_4]^T = [x, \theta, \dot{x}, \dot{\theta}]^T$ and u is the control input which controls the linear velocity of the cart. The objective is to steer the initial state of the cart to an upright position. We set $T = 0.005$. Fig. (5) shows the convergence of the trajectories starting from a set of ten randomly selected initial conditions to the origin when a stabilizing feedback controller is applied to the unknown nonlinear system.

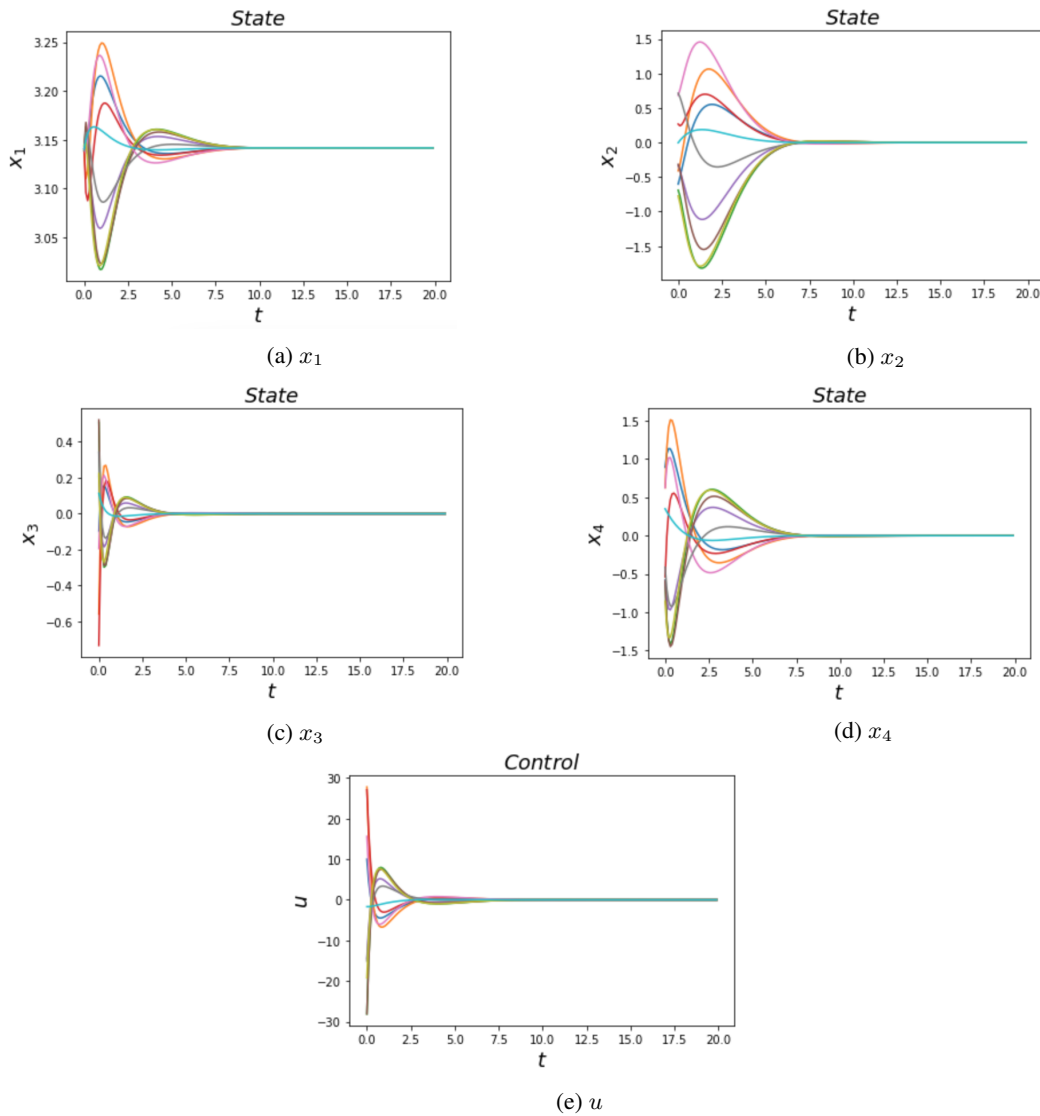


Figure 5: The evolution of the state and control input with time for the cart pole system

4.4 Spacecraft rendezvous operation

Last, we consider the spacecraft rendezvous operation whose governing equations are given by the Hill Clohessy Wiltshire (HCW) equations as follows:

$$\ddot{x} = 3n^2x + 2n\dot{y} + u_1, \quad \ddot{y} = -2n\dot{x} + u_2 \quad (31)$$

where $\mathbf{x} = [x, y, \dot{x}, \dot{y}]^T$, $\mathbf{u} = [u_1, u_2]^T$, $n = \sqrt{\mu/a^3}$, $a = 6793137$ (low earth orbit) is the length of the semi-major axis, $\mu = 3.986 \times 10^{14}$ is the gravitational constant. For more details on the HCW model, the reader may refer to [56]. We set $T = 0.005$. Figs. 6a-6d shows the evolution of the closed-loop trajectories starting from initial conditions which are sampled uniformly from $[-10, 10]^4$. Figs. 6e and 6f shows the evolution of stabilizing feedback control inputs for the rendezvous problem.

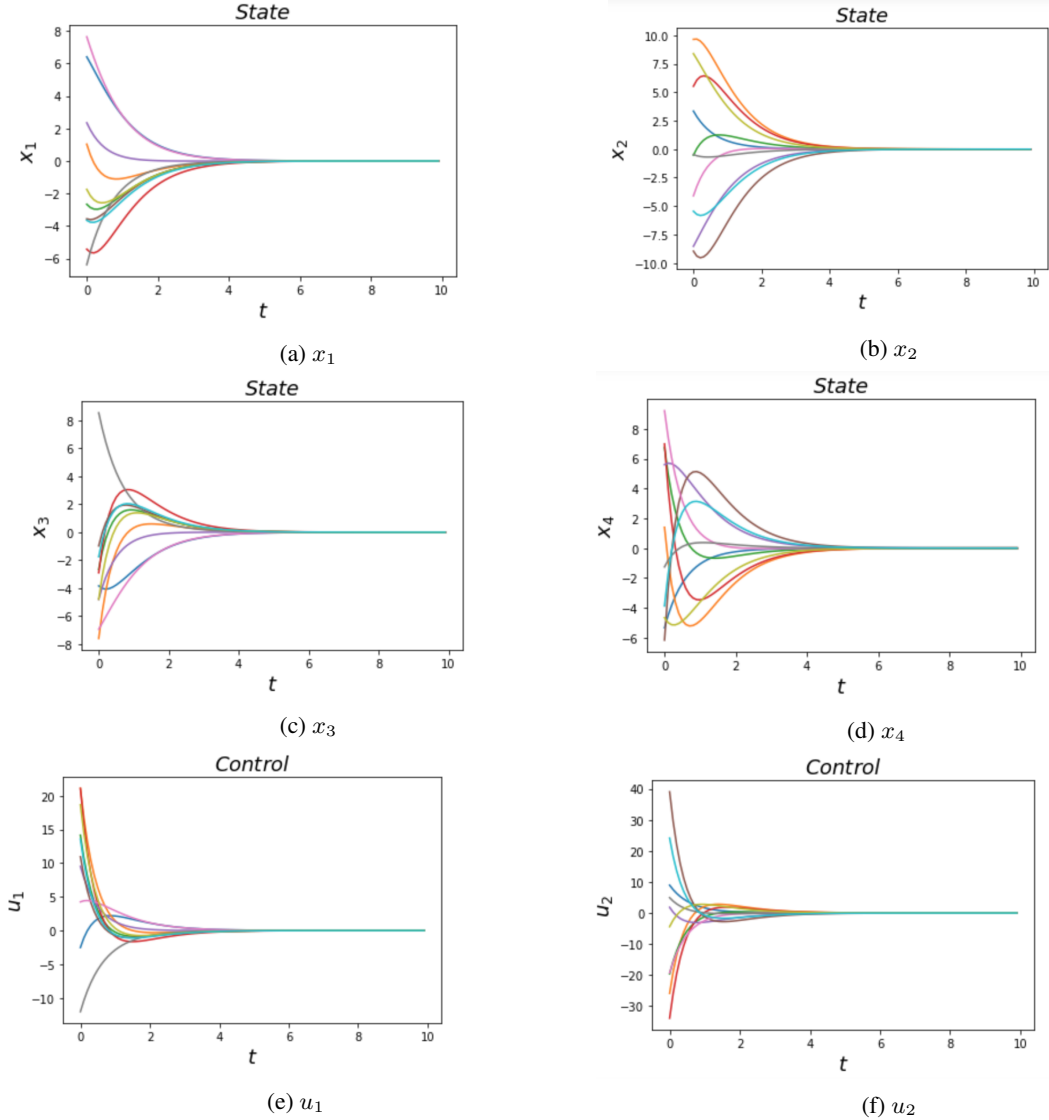


Figure 6: The evolution of the state and control input with time for the spacecraft rendezvous operation

Remark 5 Note that depending on the complexity of the system dynamics, the dimension of the lifted space N can be increased or decreased. Further, it was observed that with increase in N , the computational time required for SMT solver to find counterexamples for computing the CLF increases.

5 Conclusions

In this paper, we propose a learning framework to compute an approximation of an unknown nonlinear system via a known higher dimensional Koopman based bilinear system and design a feedback controller via the learned Control Lyapunov Function (CLF) to ensure closed-loop asymptotic stability. Our approach simultaneously learns the matrices governing the bilinear system, Koopman based observables and a valid CLF using a learner and a falsifier. The learned CLF is then used to design a stabilizing feedback controller for the unknown nonlinear system. Numerical experiments are provided to validate that our proposed class of stabilizing feedback controllers based on the learned CLF is able to steer the unknown nonlinear system to the final desired state. A particularly exciting direction for our future work is to use the learned bilinear model to design robust control laws which can account for disturbances acted upon the system as well as modelling uncertainties and also extend the results proposed herein to stochastic nonlinear control systems. Further, we plan to validate our work on complex real world physical systems.

Acknowledgments

This research has been supported in part by NSF award CMMI-1937957.

References

- [1] Kevin K Chen, Jonathan H Tu, and Clarence W Rowley. Variants of dynamic mode decomposition: boundary condition, koopman, and fourier analyses. *Journal of nonlinear science*, 22(6):887–915, 2012.
- [2] Jonathan H Tu. *Dynamic mode decomposition: Theory and applications*. PhD thesis, Princeton University, 2013.
- [3] Milan Korda and Igor Mezić. On convergence of extended dynamic mode decomposition to the koopman operator. *Journal of Nonlinear Science*, 28(2):687–710, 2018.
- [4] Matthew O Williams, Maziar S Hemati, Scott TM Dawson, Ioannis G Kevrekidis, and Clarence W Rowley. Extending data-driven koopman analysis to actuated systems. *IFAC-PapersOnLine*, 49(18):704–709, 2016.
- [5] Ian Abraham and Todd D Murphey. Active learning of dynamics for data-driven control using koopman operators. *IEEE Transactions on Robotics*, 35(5):1071–1083, 2019.
- [6] Daniel Bruder, Xun Fu, R Brent Gillespie, C David Remy, and Ram Vasudevan. Data-driven control of soft robots using koopman operator theory. *IEEE Transactions on Robotics*, 37(3):948–961, 2020.
- [7] Giorgos Mamakoukas, Maria Castano, Xiaobo Tan, and Todd Murphey. Local koopman operators for data-driven control of robotic systems. In *Robotics: science and systems*, 2019.
- [8] Giorgos Mamakoukas, Maria L Castano, Xiaobo Tan, and Todd D Murphey. Derivative-based koopman operators for real-time control of robotic systems. *IEEE Transactions on Robotics*, 2021.
- [9] Vrushabh Zinage and Efstathios Bakolas. Koopman operator based modeling for quadrotor control on se (3). *IEEE Control Systems Letters*, 2021.
- [10] Milan Korda, Yoshihiko Susuki, and Igor Mezić. Power grid transient stabilization using koopman model predictive control. *IFAC-PapersOnLine*, 51(28):297–302, 2018.
- [11] Yoshihiko Susuki and Igor Mezić. Nonlinear koopman modes and power system stability assessment without models. *IEEE Transactions on Power Systems*, 29(2):899–907, 2013.
- [12] Amit Surana, Matthew O Williams, Manfred Morari, and Andrzej Banaszuk. Koopman operator framework for constrained state estimation. In *2017 IEEE 56th Annual Conference on Decision and Control (CDC)*, pages 94–101. IEEE, 2017.
- [13] Marcos Netto and Lamine Mili. A robust data-driven koopman kalman filter for power systems dynamic state estimation. *IEEE Transactions on Power Systems*, 33(6):7228–7237, 2018.
- [14] Hyungjin Choi, Umesh Vaidya, and Yongxin Chen. A convex data-driven approach for nonlinear control synthesis. *Mathematics*, 9(19):2445, 2021.
- [15] Carl Folkestad, Yuxiao Chen, Aaron D Ames, and Joel W Burdick. Data-driven safety-critical control: Synthesizing control barrier functions with koopman operators. *IEEE Control Systems Letters*, 5(6):2012–2017, 2020.
- [16] Debdipta Goswami and Derek A Paley. Bilinearization, reachability, and optimal control of control-affine nonlinear systems: A koopman spectral approach. *IEEE Transactions on Automatic Control*, 2021.

- [17] Bowen Huang, Xu Ma, and Umesh Vaidya. Feedback stabilization using koopman operator. In *2018 IEEE Conference on Decision and Control (CDC)*, pages 6434–6439. IEEE, 2018.
- [18] S Sinha, U Vaidya, and R Rajaram. Operator theoretic framework for optimal placement of sensors and actuators for control of nonequilibrium dynamics. *Journal of Mathematical Analysis and Applications*, 440(2):750–772, 2016.
- [19] Vrushabh Zinage and Efstathios Bakolas. Far-field minimum-fuel spacecraft rendezvous using koopman operator and l 2/l 1 optimization. In *2021 American Control Conference (ACC)*, pages 2992–2997. IEEE, 2021.
- [20] Vrushabh Zinage and Efstathios Bakolas. Koopman operator based modeling and control of rigid body motion represented by dual quaternions. *arXiv preprint arXiv:2110.04967*, 2021.
- [21] Alexander Broad, Todd Murphey, and Brenna Argall. Learning models for shared control of human-machine systems with unknown dynamics. *arXiv preprint arXiv:1808.08268*, 2018.
- [22] Abhinav Narasingam and Joseph Sang-II Kwon. Koopman lyapunov-based model predictive control of nonlinear chemical process systems. *AIChE Journal*, 65(11):e16743, 2019.
- [23] Bethany Lusch, J Nathan Kutz, and Steven L Brunton. Deep learning for universal linear embeddings of nonlinear dynamics. *Nature communications*, 9(1):1–10, 2018.
- [24] Fletcher Fan, Bowen Yi, David Rye, Guodong Shi, and Ian R Manchester. Learning stable koopman embeddings. *arXiv preprint arXiv:2110.06509*, 2021.
- [25] Masih Haseli and Jorge Cortés. Fast identification of Koopman-invariant subspaces: parallel symmetric subspace decomposition. In *2020 American Control Conference (ACC)*, pages 4545–4550, 2020.
- [26] Masih Haseli and Jorge Cortés. Learning koopman eigenfunctions and invariant subspaces from data: symmetric subspace decomposition. *IEEE Transactions on Automatic Control*, 2021.
- [27] Masih Haseli and Jorge Cortés. Parallel learning of Koopman eigenfunctions and invariant subspaces for accurate long-term prediction. *IEEE Transactions on Control of Network Systems*, 2021.
- [28] Eduardo D Sontag. A ‘universal’ construction of artstein’s theorem on nonlinear stabilization. *Systems & control letters*, 13(2):117–123, 1989.
- [29] Zvi Artstein. Stabilization with relaxed controls. *Nonlinear Analysis: Theory, Methods & Applications*, 7(11):1163–1173, 1983.
- [30] Graziano Chesi and Didier Henrion. Guest editorial: Special issue on positive polynomials in control. *IEEE Transactions on Automatic Control*, 54(5):935–936, 2009.
- [31] Didier Henrion and Andrea Garulli. *Positive polynomials in control*, volume 312. Springer Science & Business Media, 2005.
- [32] Zachary Jarvis-Wloszek, Ryan Feeley, Weehong Tan, Kunpeng Sun, and Andrew Packard. Some controls applications of sum of squares programming. In *42nd IEEE international conference on decision and control (IEEE Cat. No. 03CH37475)*, volume 5, pages 4676–4681. IEEE, 2003.
- [33] Anirudha Majumdar and Russ Tedrake. Funnel libraries for real-time robust feedback motion planning. *The International Journal of Robotics Research*, 36(8):947–982, 2017.
- [34] Amir Ali Ahmadi, Miroslav Krstic, and Pablo A Parrilo. A globally asymptotically stable polynomial vector field with no polynomial lyapunov function. In *2011 50th IEEE Conference on Decision and Control and European Control Conference*, pages 7579–7580. IEEE, 2011.
- [35] George Cybenko. Approximation by superpositions of a sigmoidal function. *Mathematics of control, signals and systems*, 2(4):303–314, 1989.
- [36] Kurt Hornik. Some new results on neural network approximation. *Neural networks*, 6(8):1069–1072, 1993.
- [37] Chang Ya-Chien, Roohi Nima, and Gao Sicun. Neural lyapunov control. In *NeurIPS*, 2019.
- [38] Arash Mehrjou, Mohammad Ghavamzadeh, and Bernhard Schölkopf. Neural lyapunov redesign. *Proceedings of the 3rd Conference on Learning for Dynamics and Control*, 2020.
- [39] Hadi Ravanbakhsh and Sriram Sankaranarayanan. Learning control lyapunov functions from counterexamples and demonstrations. *Autonomous Robots*, 43(2):275–307, 2019.
- [40] Wanxin Jin, Zhaoran Wang, Zhuoran Yang, and Shaoshuai Mou. Neural certificates for safe control policies. *arXiv preprint arXiv:2006.08465*, 2020.
- [41] Alessandro Abate, Daniele Ahmed, Mirco Giacobbe, and Andrea Peruffo. Formal synthesis of lyapunov neural networks. *IEEE Control Systems Letters*, 5(3):773–778, 2020.

- [42] Hongkai Dai, Benoit Landry, Lujie Yang, Marco Pavone, and Russ Tedrake. Lyapunov-stable neural-network control. *Robotics: Science and Systems*, 2021.
- [43] Nicholas M Boffi, Stephen Tu, Nikolai Matni, Jean-Jacques E Slotine, and Vikas Sindhwani. Learning stability certificates from data. *Conference on Robot Learning*, 2020.
- [44] Spencer M Richards, Felix Berkenkamp, and Andreas Krause. The lyapunov neural network: Adaptive stability certification for safe learning of dynamical systems. In *Conference on Robot Learning*, pages 466–476. PMLR, 2018.
- [45] Héctor J Sussmann. Semigroup representations, bilinear approximation of input-output maps, and generalized inputs. In *Mathematical systems theory*, pages 172–191. Springer, 1976.
- [46] Bernard O Koopman. Hamiltonian systems and transformation in hilbert space. *Proceedings of the national academy of sciences of the united states of america*, 17(5):315, 1931.
- [47] Debdipta Goswami and Derek A Paley. Global bilinearization and controllability of control-affine nonlinear systems: a koopman spectral approach. In *2017 IEEE 56th Annual Conference on Decision and Control (CDC)*, pages 6107–6112. IEEE, 2017.
- [48] John Charles Butcher. *The numerical analysis of ordinary differential equations: Runge-Kutta and general linear methods*. Wiley-Interscience, 1987.
- [49] Steven L Brunton, Bingni W Brunton, Joshua L Proctor, and J Nathan Kutz. Koopman invariant subspaces and finite linear representations of nonlinear dynamical systems for control. *PloS one*, 11(2):e0150171, 2016.
- [50] Daniel Bruder, Xun Fu, and Ram Vasudevan. Advantages of bilinear koopman realizations for the modeling and control of systems with unknown dynamics. *IEEE Robotics and Automation Letters*, 6(3):4369–4376, 2021.
- [51] Eduardo D Sontag. A lyapunov-like characterization of asymptotic controllability. *SIAM journal on control and optimization*, 21(3):462–471, 1983.
- [52] Sicun Gao, Soonho Kong, and Edmund M Clarke. dreal: An smt solver for nonlinear theories over the reals. In *International conference on automated deduction*, pages 208–214. Springer, 2013.
- [53] Hassan K Khalil. *Nonlinear systems*. 2017.
- [54] Dimitrios Pylorof and Efstathios Bakolas. Stabilization of input constrained nonlinear systems with imperfect state feedback using sum-of-squares programming. In *2018 IEEE Conference on Decision and Control (CDC)*, pages 1847–1852. IEEE, 2018.
- [55] Dimitrios Pylorof and Efstathios Bakolas. Analysis and synthesis of nonlinear controllers for input constrained systems using semidefinite programming optimization. In *2016 American Control Conference (ACC)*, pages 6959–6964. IEEE, 2016.
- [56] Howard Curtis. *Orbital mechanics for engineering students*. Butterworth-Heinemann, 2013.